Title
Scanning electron microscopy of otic capsule and calvarial bone ablated by a holmium-YAG laser

Journal
Lasers in Medical Science, 9(4)

ISSN
0268-8921

Authors
Wong, Brian JF
Liaw, Lih-Huel L
Neev, Joseph
et al.

Publication Date
1994-12-01

DOI
10.1007/bf02593887

Lasers in Medical Science 1994, 9:249–260

Scanning Electron Microscopy of Otic Capsule and Calvarial Bone Ablated by a Holmium-YAG Laser

BRIAN J.F. WONG[a,b], LIH-HUEI L. LIAW[a], JOSEPH NEEV[a], MICHAEL W. BERNS[a]

[a]*Beckman Laser Institute and Medical Clinic, University of California, Irvine, 1002 Health Sciences Road East, Irvine, CA 92715, USA*

[b]*Department of Otolaryngology–Head and Neck Surgery, University of California, Irvine, 101 The City Drive, Orange, CA 92668, USA*

Correspondence to Dr B.J.F. Wong, Beckman Laser Institute, University of California, 1002 Health Sciences Road East, Irvine, CA 92715, USA

Paper received 12 November 1994

Abstract. Scanning electron microscopy (SEM) was performed on holmium-YAG laser ablated bone in order to study the surface morphology of the ablation crater. An otosurgical bone model of porcine otic capsule and calvarial cortical bone was used. Otic capsule bone is dense and homogeneous whereas cortical bone is porous. Both bone tissues were studied under fresh and dehydrated conditions to investigate the role of water in the ablation process. Laser irradiation time was varied from 5 to 60 s. Laser flux was 85 mJ pulse^{-1} at 4-Hz pulse repetition rate. Globular spheroids of melted bone material were noted in both wet and dried specimens for both tissues. Several of these globules ruptured yielding an SEM image which suggests a violent ejection process. SEMs of dry cortical bone demonstrated the presence of fibres which reflect the selective removal of inorganic surface bone constituents with preservation of subsurface residual collagen fibres. The ablation crater walls in wet tissues appear rougher and possibly reflect a more violent ablation process due to water vaporization causing expulsion of bone material. In contrast, the crater walls in dry tissue appear smoother.

INTRODUCTION

Lasers have gained widespread acceptance in otological surgery, and have become the standard of practice in the treatment of ossicular chain disorders such as otosclerosis, a disease of bone resorption and remodelling affecting the otic capsule in the temporal bone. Following the successful introduction of the laser in stapedotomy surgery in 1980 (1), three lasers have gained wide acceptance in ear surgery. Commercially available CO_2, argon, and KTP (Nd-YAG) laser systems dominate clinical practice (2–7). Each of these wavelengths has its own advantages and drawbacks. However, clinical practice has not kept pace with the development of new laser systems. This is particularly true with respect to other infra-red wavelengths.

The holmium-YAG laser has been advocated for use in otosclerosis and other chronic ear disease operations (8–10). The main advantage of this wavelength (2.12 μm) is that it has a high peak of absorption in water as well as in bone relative to visible wavelength lasers. Furthermore, it is easily transmitted with readily available flexible quartz fibres. While the ablative properties of Ho-YAG lasers are well known (11), there are no studies which specifically address the laser-tissue interactions of this wavelength in a bone model that reflects conditions encountered during middle-ear surgery.

The bone surrounding the structures of the inner ear is unique and embryologically distinct (12). This bone is called endochondral bone and forms the otic capsule. It is essentially mature at 9–12 weeks gestation. It is a primitive form of bone with dense extracellular matrix components. It is also the hardest and densest bone in the human body and microsurgery in this region requires small diamond drill bits. The footplate of the stapes bone is derived from otic capsule material and

0268–8921/94/040249+12 $08.00/0

in pathological states such as otosclerosis the footplate may be exceptionally dense, thickened, and fixed to the surrounding oval window. In non-pathological conditions, the stapes bone moves up and down within the oval window like a piston and is part of the ossicular mechanisms transmitting sound to the inner ear. The remaining bone tissues in the middle ear (ossicles) and temporal bone (mastoid cavity) are more similar to cortical and lamellar bone both embryologically and histologically. The stapedotomy operation is a procedure where a hole approximately 500 μm in diameter is drilled through the entire footplate of the stapes. Then a prosthetic piston is inserted to reconstruct a functional ossicular chain and replace a non-functional and fused stapes bone. In this situation, the underlying histopathology is characterized by extremely dense and acellular bone (sclerotic phase) or relatively cellular and vascular tissue (spongiotic phase) (13). There is no animal model which reflects this process.

Otic capsule is extremely dense and with little porosity in terms of its microarchitecture. The surface of this bone is smooth and marble-like. In contrast, cortical bone (substantia compacta) is punctuated by pockets of fluid and cellular material. The honeycombed structure of cortical bone provides excellent mechanical strength with a substantial reduction in bone weight per unit volume. Cortical bone and lamellar bone (substantia spongiosa) are the two bone types forming the calvarial vault (14). Preliminary investigations on the ablation process in porcine otic capsule and cortical bone have revealed some startling findings. Otic capsular tissue under physiological conditions (wet) ablates with relatively consistent ablation pattern (15) with limited episodes of 'stalled out' ablation. The 'stalling out' phenomena is where ablation begins but ceases despite continued irradiation (16); the mechanism of action is thought to be a combination of total tissue desiccation (17) and possibly surface modification of the tissue. In wet tissue, while the ablation rate is lower than in dry tissue, ablation through a section of the homogeneous, non-porous otic capsule bone proceeds in a very regular fashion. The ablation rate assumes a linear dependence as a function of fluence, albeit with poor correlation. In contrast, with dehydrated otic capsule, this regularity in the ablation process is not observed. Some dehydrated specimens ablate readily and then ablation ceases despite continued laser irradiation. Some specimens do not show any evidence of an ablation crater and the only surface feature is a small patch of carbonized bone material despite several minutes of continuous pulsed laser irradiation. The fluence at which consistent ablation occurs is higher in the dry otic tissue than the wet.

Water appears to influence the ablation process in both otic capsule and cortical bone and may play a key role in the initiation and continuation of regular ablation (17). Dentin shares many of the same ablation characteristics as otic capsule bone under both wet and dehydrated conditions (18). Dentin is the main component forming the central substance of a tooth. It is extremely hard with little macroscopically visible porosity and appears similar to otic tissue under low-power light microscopy. In vitro, wet dentin ablates with a marked increase in regularity than dehydrated dentin (19). In contrast, in wet and dehydrated cortical tissue, ablation proceeded in a very regular manner (20). Notably, ablation in dehydrated cortical bone proceeded at a much faster rate than in its wet (physiologic) counterpart. This is reflected by the differences in the ablation rate. In an attempt to gain insight into the actual mechanisms of ablation in these tissues, scanning electron microscopy (SEM) was performed. While the SEM characteristics of the human stapes are well defined (21–24), the interaction of laser energy with the otic-derived tissue of the stapes footplate is largely unexplored (25, 26).

In this study, the effect of Ho-YAG laser irradiation on calvarial and otic capsule bone tissue is examined in terms of SEM findings. First, the effect of increasing the number of laser pulses (reflected by exposure time) is studied in the crater base and crater wall of these tissues. Second, these same structures are assessed under similar conditions in chemically dehydrated tissues to investigate the role of water in the ablation process.

MATERIALS AND METHODS

Cortical and lamellar bones were harvested from the parietal and frontal bones of freshly killed domestic pigs, obtained from a large regional packing company (Clougherty Packing Company, Vernon, California). Soft tissues were gently removed from the calvarial surfaces. An industrial plug cutter (Irwin Co., Model 43904 Wilmington, Ohio) was used to

obtain 0.5-in cylindrical cores of bone tissue that included both internal and external cortical surfaces. A low-speed microstructural saw with a diamond wafering blade (Buehler, Model 11-1180 Isomet, Lake Bluff, Illinois) was used to machine the cylinder of bone into individual discs of uniform thickness varying from 0.85 to 0.95 mm. Care was taken to precisely remove cortical bone from the outer table of the cylindrical bone plug in order to obtain a specimen of as uniform density as possible. For lamellar bone, the cylinder was machined in its midsection to ensure that no cortical bone remnants were included with these specimens. No tissue was harvested from the cortical surface that abutted the dura mater.

For fresh tissue studies, the discs were placed in a cold saline bath at 4 °C. They were used within 24 h and allowed to equilibrate with ambient temperature in a 25 °C saline bath. For dry tissue investigations, the tissue was first fixed in formaldehyde for 24 h, then serially dehydrated with graded alcohol solutions from 30 to 100%. The tissue was preserved in formaldehyde to necessitate safe storage and handling. Each individual disc was inspected for uniformity in thickness using a micrometer and evaluated visually with a low-power microscope to ensure gross uniformity. Specimens with marked heterogeneity (e.g. suture lines, cracks) were discarded.

Otic capsule tissue was removed from the temporal bone of the fresh pig skull. A large calvarial craniotomy was created with a bone saw. The otic capsule in the domestic pig is separate from the rest of the temporal bone and a very clear demarcation in the suture line exists. The otic capsule tissue is noticeably more yellow and smoother than the surrounding petrous tissue. It is easily prised loose with a narrow osteotome. Fresh otic capsule bone was stored in saline at 4 °C and used within 24 h. For dry tissue studies, fixation and dehydration were performed as described for lamellar and cortical tissue. Following completion of ablation, all fresh tissue was fixed in formaldehyde and serially dehydrated as described above.

A Q-switched Ho-YAG laser (λ=2.1 mm, pulse width 250 ms FWHM) was used to perform all ablation studies (Schwartz Electro-Optics Laser 1-2-3, Orlando, Florida). Pulse repetition rate was maintained at 4 Hz while energy delivered per pulse was 85 ± 5 mJ. The beam was focused with a standard CaF_2 lens with a focal length of 6 in. Spot size was determined using thermal paper and maintained at 1 mm^2. Bone speciments were held in place with a caliper mounted on an x-y-z adjustable support. Energy output from the laser was monitored with a joule meter (Gentec Model ED-500, Canada). Ablation times at this frequency were varied from less than 5 s to over 60. Several specimens were irradiated until a hole was created across the entire width of the specimen. In these specimens, irradiation was terminated by the registration of energy on the joule meter placed behind the specimen.

Following laser irradiation, fresh tissue specimens underwent fixation over 24 h with 10% formaldehyde, followed dehydration with serially graded alcohol baths. Both fresh (fixed and dehydrated) and dehydrated specimens were mounted on a stub using colloidal silver liquid (Ted Pella, Redding, California) with laser-treated areas pointing upward. These specimens were gold-coated on a PAC-1 Pelco advanced coater 9500 (Ted Pella). Micrographs were taken on a Philips 515 (Mohawk, New Jersey) scanning electron microscope at 75, 120, 500 and 1000 power magnification.

RESULTS

Dry versus wet otic capsule

At low-power magnification, the ablation craters in physiological (wet) and dehydrated otic capsule possess the common feature of extremely rough and jagged walls without any surface features suggestive of molten bone. This is illustrated in Fig. 1(a) which depicts the ablation crater in wet otic capsule bone after 24 s of laser irradiation. The walls of the craters in fresh bone appear slightly more jagged and irregular in terms of texture. In addition, these observations were also noted at several different laser exposure times (32, 24, 12 and 11 s for wet tissue). At these low-power magnifications, molten roughly spherical globules of bone (approximately 10 μm in diameter) are discernible in the crater bases of both wet and dehydrated ablated tissue [Fig. 1(b, c)].

A difference is observed in the dehydrated specimens; there is a large region of different colour and texture rimming the ablation crater in the dehydrated otic capsule [Fig. 1(c, d)] that is clearly absent in wet tissue specimens. This circumferential banding of the ablation

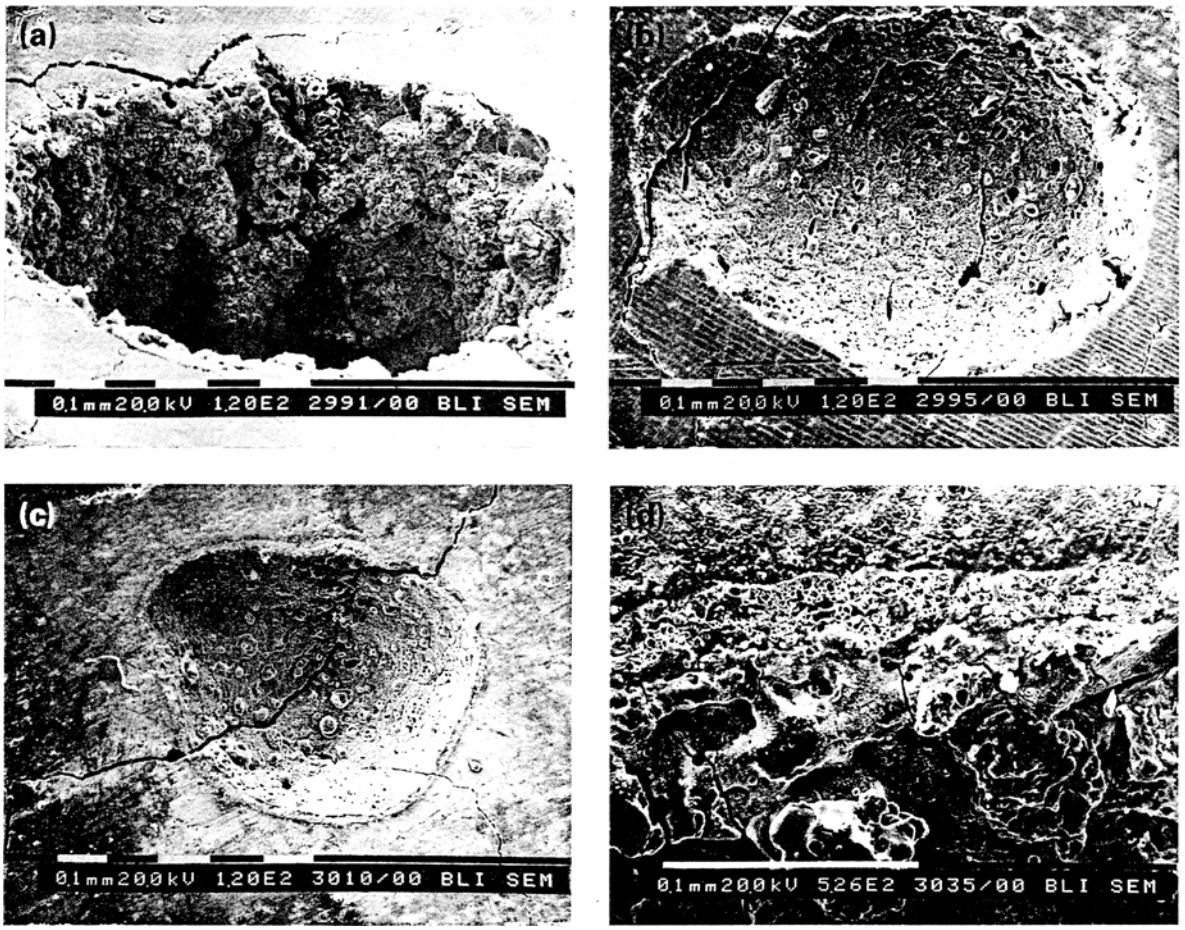

Fig. 1. (a) Ablation crater in wet otic capsule bone following 24 s of laster irradiation (magnification 120×). (b) Overhead view of ablation crater in wet otic capsule following 12 s of laser irradiation. Note the presence of molten spheroids of bone in the crater base (magnification 120×). (c) Overhead view of ablation crater in dehydrated otic capsule following 28 s of irradiation. Molten spheroids of bone are also seen in the crater base along with a thin rim of different textured tissue at the crater margins (magnification 120×). (d) High-power examination of the ablation crater rim in dehydrated otic capsule bone following 60 s of irradiation demonstrating a circumferential band approximately 0.025 mm in thickness at the crater rim (magnification 500×). All parts (a–d) reproduced at 65%.

crater measures approximately 25 μm in thickness and is well demarcated. This may reflect partial ablation occurring in the dry tissue. At 500 power magnification, more fractures across the surface of the crater base are seen in dry otic capsule [Fig. 2(a)]. Of note, in the crater bases of both wet and dry otic capsule, small pores are uniformly distributed in the matrix of melted bone [Fig. 2(a, b)]. These pores may be a byproduct of the melting of bone that occurs on the surface of the ablation crater, and may reflect the escape of vapours from beneath this molten surface. Of note, the pores distributed in the melted bone matrix of fresh otic bone appear larger in size and in greater number than compared to the pores observed in dehydrated otic tissue.

At 1000 power magnification, the bases of ablation craters were scanned and photographed with the electron microscope for dry and wet otic capsule specimens. Wet (physiological) specimens were treated for 11 or 12 s, while dry specimens were ablated for 28 and 60 s. At this high magnification, common features in the crater base included (i) the presence of smooth surface with melted bone matrix, (ii) large globules of molten bone matrix (collagen and hydroxyapetite) and (iii) large globular structures that appear to be vapour filled or ruptured [Fig. 2(c, d)]. At this magnification, the subtle difference in pore size at the crater bases between wet otic capsule and dry tissue is demonstrated [Fig. 2(d)].

Examination of the crater wall at higher power magnification reveals even greater differences between wet and dehydrated tissue. In physiological otic capsule, the crater wall after 11 s of exposure appears melted and smooth with few features suggestive of an explosive mechanism of tissue destruction. At

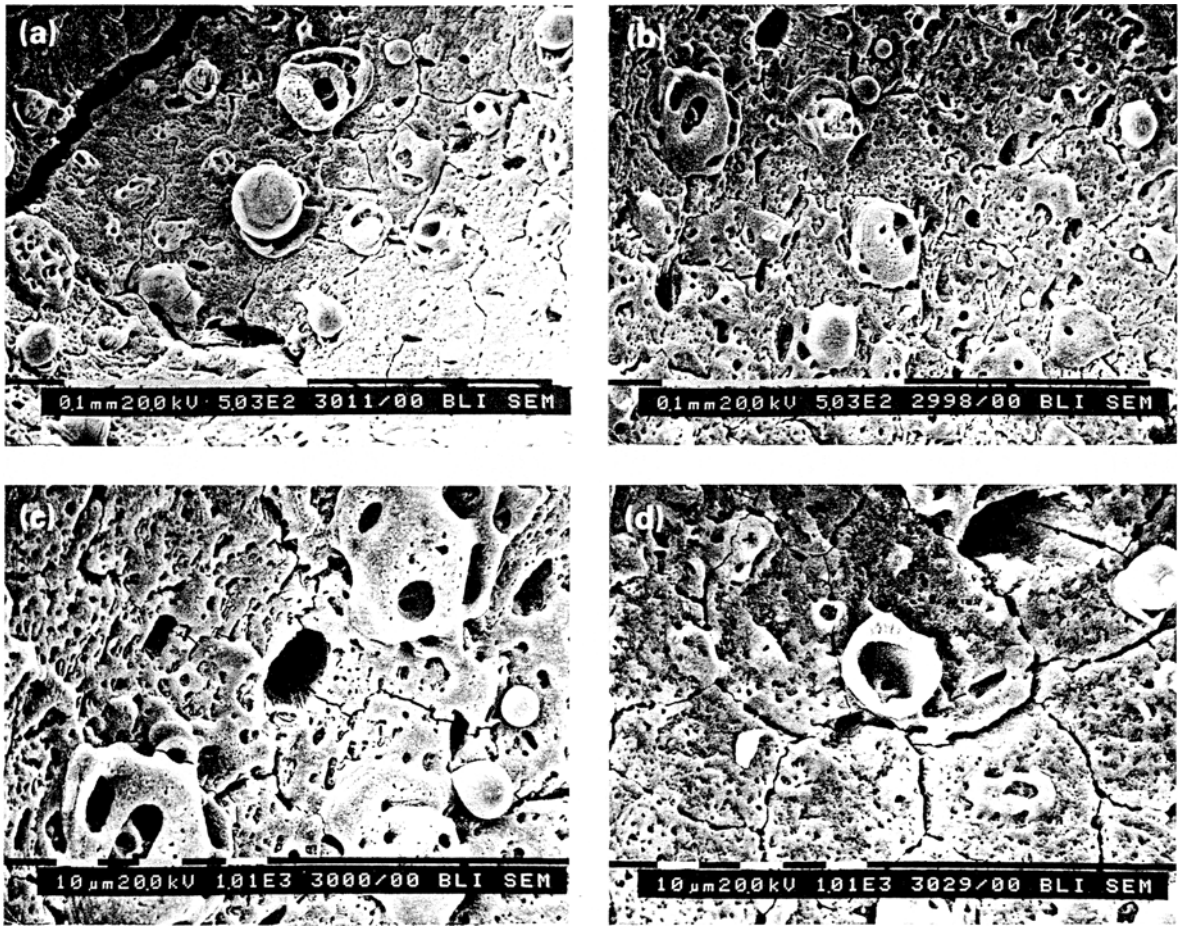

Fig. 2. (a) Fractures and small pores are seen in the crater base of dehydrated otic capsule bone following 28 s of irradiation (magnification 500×). (b) No fractures were noted in the bases of wet otic capsule bone as illustrated in this specimen treated for 12 s. The pores seen in wet otic tissue appear larger in size than those observed in dehydrated tissue (magnification 500×). (c) At higher magnification, wet otic capsule shows the presence of smooth melted bone surfaces and large globular structures. Here the specimen was treated for 12 s (magnification 1000×). (d) Dehydrated otic capsule bone shows similar features. Several structures appear to have resulted from the rupturing of a vapour-filled globule of melted bone matrix. Notably, the subtle differences in pore size in the crater base between wet and dehydrated tissue are clearly observed (magnification 1000×). All parts (a–d) reproduced at 65%.

24 s, the walls of the crater appear as if pieces of bone have been chipped off [Fig. 3(a)]. The appearance is extremely irregular with jagged and coarse features. This very irregular surface is suggestive of melting and popping of crater wall constituents with the violent expulsion of material. At 32 s, the wall of the crater appears rougher in texture than at 24 s (wet) [Fig. 3(b)]. These characteristics are not visible with shorter irradiation times as evidenced by the smooth features seen at 11 s [Fig. 3(c)]. In contrast, dehydrated otic capsule at prolonged irradiation times (28 and 60 s exposure), produces crater wall surfaces that are much smoother and uniform than their physiological counterparts, as illustrated in Fig. 3(d) for 28 s of exposure. Notably, numerous spheroid globules of molten material appear on the crater walls at 28 s. This suggests the melting of the dense otic bone matrix. High-power examination of dry otic tissues at 28 and 60 s does not show the irregularity and coarseness of surface features seen in ablated wet otic tissues. More melted and smooth surfaces are clearly evident [Fig. 3(d)].

Dry versus wet cortical bone

The crater base of dehydrated cortical bone at 5, 10 and 15 s and physiological cortical bone 5, 10 and 15 s laser exposure were examined at 120 power magnification. After 5 s of laser exposure, several interesting features are noted. First, the surface of dehydrated cortical bone has a fine lattice-like surface with an appearance suggestive of exposed collagen fibres in the absence of inorganic bony matrix

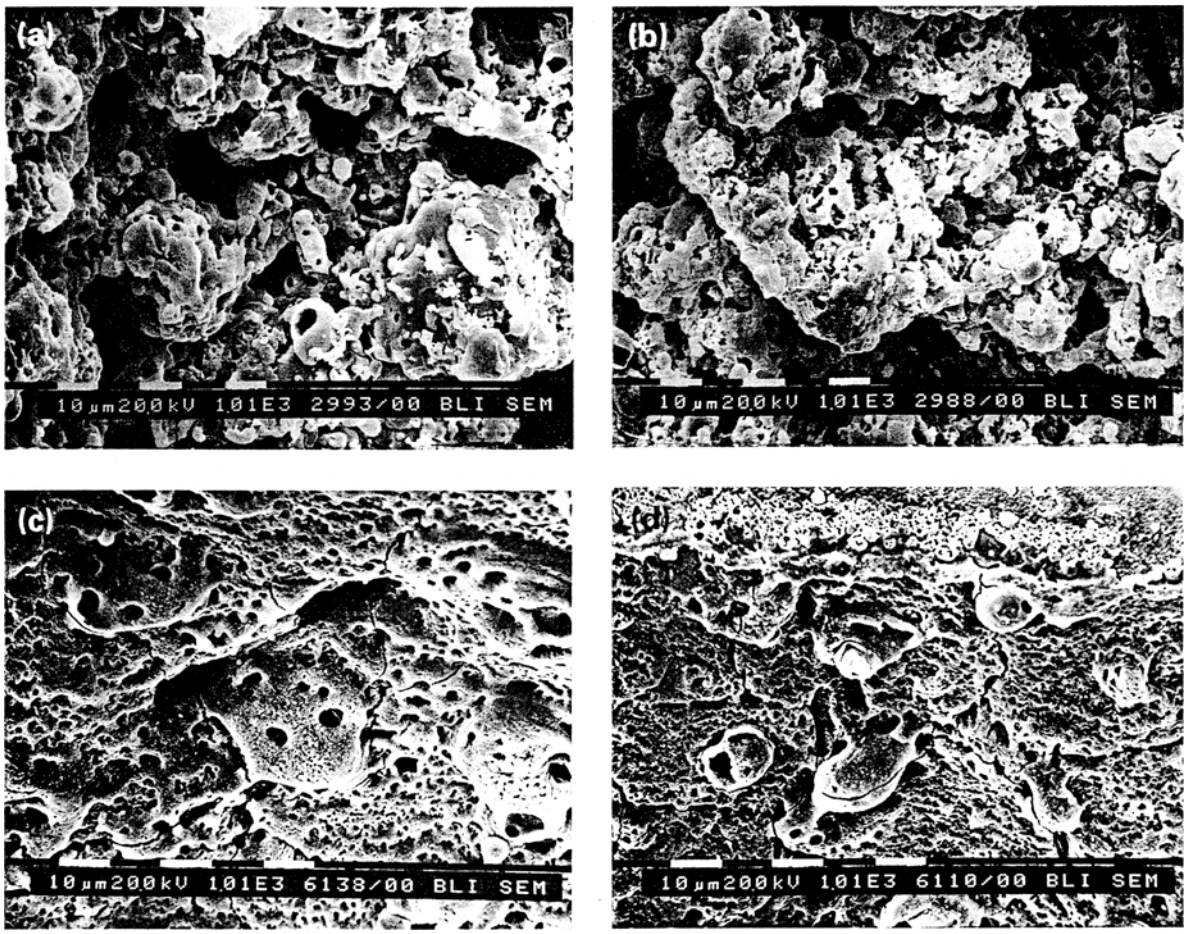

Fig. 3. (a) The crater wall in wet otic capsule following 24 s of irradiation is irregular and jagged. This suggests an eruptive and violent mechanism of tissue destruction (magnification 1000×). (b) Following 32 s of irradiation, the crater wall in wet otic capsule tissue appears even coarser in texture than observed at 24 s (magnification 1000×). (c) At a shorter irradiation interval, smooth surface features are clearly observed, here illustrated in wet otic capsule following 12 s of laser irradiation (magnification 1000×). (d) In dehydrated otic capsule the walls of the ablation crater are smooth despite 28 s of treatment. Numerous spheroid globules of molten bone material are observed along the crater wall. All parts (a–d) reproduced at 65%.

[Fig. 4(a)]. In physiological cortical bone, 5 s of laser exposure creates an ablation crater with undulating waves of molten bone oriented concentrically towards the centre of the crater [Fig. 4(b)]. Also of note is the much larger size of the ablation crater in the dry tissue [Fig. 4(a)] compared with wet tissue [Fig. 4(b)]. Both craters were produced by the same laser at identical fluence, pulse repetition rate, and laser exposure. The larger crater size in the dehydrated tissue suggests that the ablation threshold for dry cortical bone is much lower than its physiological (wet) counterpart. Indeed in direct ablation rate measurements, the lower ablation threshold of dry cortical tissue was confirmed (18).

After 10 s of exposure, the mesh/lace surface appearance of dry tissue is no longer present [Fig. 4(c)]. In both wet and dry tissue, the formation of globular bone spheres occurs and is readily observed [Fig. 4(c, d)]. The globule size in dry cortex appears to be larger. At 15 s, the craters in both tissues look very similar, with the exception that the globules in the dry cortical tissue are larger. This subtle difference in size noted in the crater bases may reflect the difference in ablation thresholds between physiological and dehydrated tissue.

At higher power magnification and 5 s laser exposure, the base of the ablation crater in physiological bone illustrates more clearly the smooth undulating waves of molten bone [Fig. 5(a)]. There is a conspicuous absence of the large (10–15 μm) globular spheres, notably there are no spheroid structures with holes in them. There are no surface features suggestive of ruptured molten globules of bone in contrast to the observations in wet bone at 10 s irradiation [Fig. 4(d)]. At 10 s in wet bone, the base of

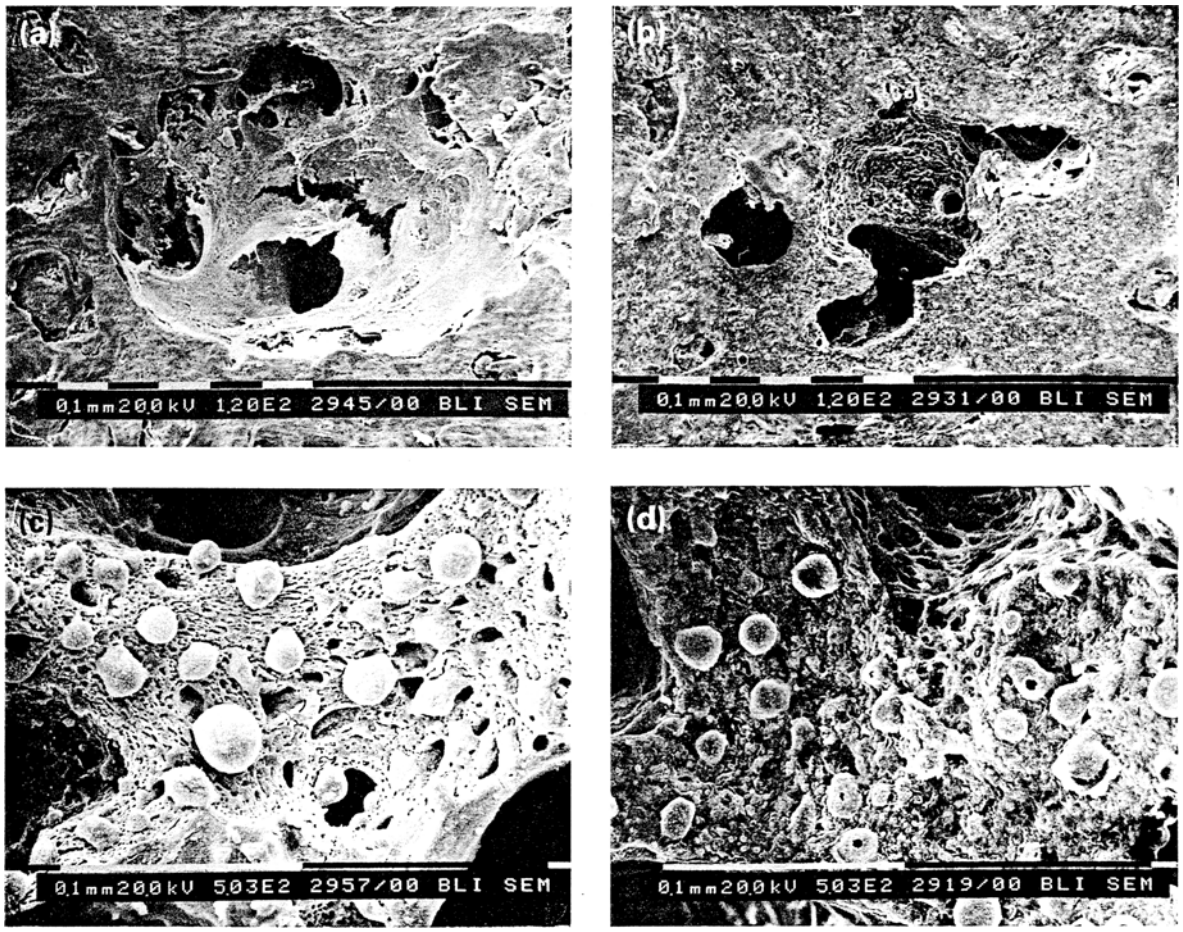

Fig. 4. (a) In dry cortical bone irradiated for 5 s of laser exposure, a fine lattice-like surface with an appearance suggestive of collagen fibres in the absence of bone matrix is visible (magnification 120×). (b) In wet cortical bone irradiated for 5 s, no lattice suggestive of collagen fibres is observed. Instead, the ablation crater is filled with undulating waves of molten bone oriented concentrically towards the centre of the crater (magnification 120×). (c) After 10 s of laser exposure in dry cortical tissue, the network of collagen fibres is no longer observed. Globular masses of molten bone are seen on the crater base (magnification 500×). (d) In wet cortical bone. 10 s of laser irradiation results in very similar features: however, several of the globular masses appear to have ruptured (magnification 500×). All parts (a–d) reproduced at 65%.

the crater takes on characteristics which include numerous large (10–15 μm) spheres of molten bone. There are several of these structures with large holes in them, and suggest the explosive release of vaporized water or collagen. The surface look less smooth and shiny. At 15 s in wet bone, there are significant similarities between wet bone at 10 s. A peripheral observation includes the findings of melted bone in the vicinity of the natural holes in the bone.

At 5 s in dry bone, ablation results in the creation of a fine mesh of structures across the base of the ablation crater that is much more clearly observed at higher powers (500, 1000 and 5000 ×). There is a web-like appearance to the surface [Fig. 5(b–d)]. This surface appearance could possibly be residual collagen from which the surrounding inorganic bone (hydroxyapetitive) material has been ablated away. At 10 s in dry cortex, the fibrous/lace-like structure seen at 5 s is absent, but there is still a perforated pattern in the base of the crater [Fig. 4(c)] reminiscent of the crater base in dry otic tissue [Fig. 2(d)]. The surface of the crater is smooth and punctuated by small pores. The presence of the molten globules is seen and they measure 10–15 μm or greater in diameter. Many of these globules are perforated, suggesting an escape of gaseous contents. At 15 s in dry cortex, there appears to be more melted bone matrix which has dripped around the natural holes in the bone matrix. The large spheres of molten bone are still present. An image of molten bone flowing down the crater is noted at 500 and 1000 power magnification [Fig. 6(a, b)].

At 1000 power magnification, wet cortical tissue at 5 s continues to reflect the same features seen at lower magnifications, undulat-

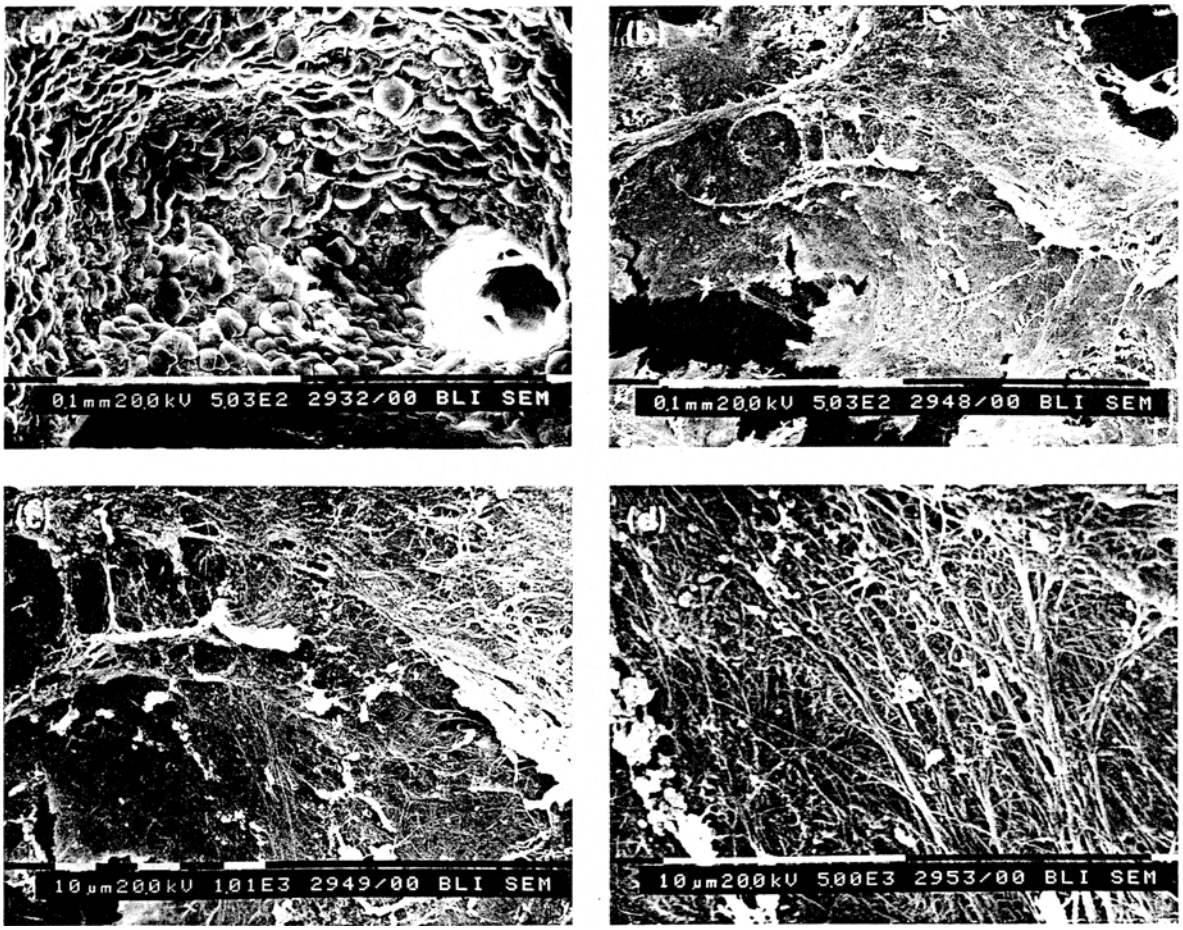

Fig. 5. (a) Higher power magnification more clearly demonstrates the undulating waves of molten bone within the ablation crater after 5 s of irradiation (magnification 500×). (b) In dry cortical bone, high-power magnification of the specimen in Fig. 4 (a) clearly reveals the presence of fibres arranged in a meshwork (magnification 500×). (c) Higher magnification of the same specimen shows the finer detail of these fibres in the dry cortical bone (magnification 1000×). (d) Fibres are clearly visible in the crater base at 5000× magnification. In hard tissue ablation, it has been reported that the organic constituents of bone ablate preferentially resulting in an increase in mineral content within the ablation site. Here, the opposite seems to have occurred as the inorganic component have been selectively ablated (magnification 5000×). All parts (a–d) reproduced at 65%.

ing waves of molten bone are clearly visible dripping down towards the centre of the ablation crater. At 10 s, the bone surface looks more disordered, large spheres of molten bone populate the landscape some appear to be caught erupting, remnant craters also appear [Fig. 6(c, d)]. This is further reflected at 15 s. High-power microscopy (5000 ×) of dry cortical bone provides a more detailed examination of the fibril numerous tendril-like structures observed at lower power [Fig. 5(d)]. A vast mesh or network of tissue is clearly evident; there are no surface features that suggest melting as a step in the ablation process at this exposure time. At 10 s, the mesh/network-like structures are no longer seen. Globular masses of molten tissue are readily apparent. It appears that there are numerous spheres of material that extend down towards the base of the crater. At 15 s, there is more evidence of melting, although this is not significantly different than findings in wet tissue. Interestingly, several images depict the melting of collagen or other bone components. Melted globules of bone are dripping down the wall of a haversian structure [Fig. 6(b)].

Serial examination of crater walls of dry and wet otic bone

At 120 power magnification, wet and dry otic capsule crater walls appear very similar, with the exception that the wet walls appear more fractured and chiselled in appearance with a rougher texture [Fig. 1(a, d)]. Higher magnification at 500 power, illustrates subtle differences in the crater wall. The differences become less clear, both dry and wet tissues have a rough surface, the wet tissue looks like

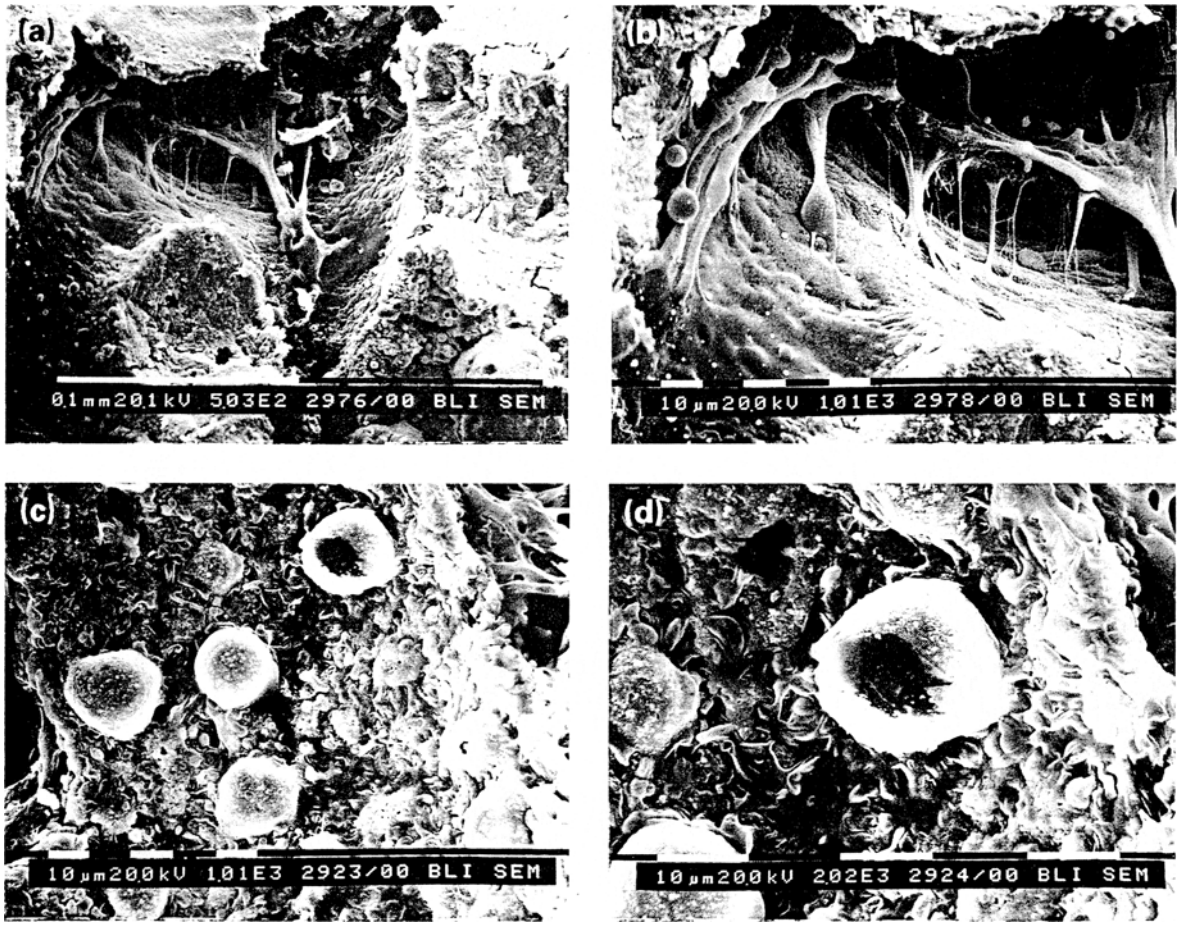

Fig. 6. (a) In dry cortical bone, molten bone matrix has dripped down the edge of an ablation crater (magnification 500×). (b) At 1000× magnification, this phenomenon is dramatically illustrated (magnification 1000×). (c) Following 10 s of irradiation, high-power magnification of the ablation crater base in west cortical bone reveals large globules of bone (magnification 1000×). (d) At 2000× magnification, a globule appears to be ruptured. This suggest that the contents of this molten mass of bone was water or vaporized organic components. All parts (a–d) reproduced at 65%.

small spheres of clay of greatly varying size thrown against a wall [Fig. 3(a)]; the dry tissue has a similar appearance, but these balls of clay have melted [Fig. 1(d)]. On gross light microscopy, these very rough structures likely correspond to carbonized bone material that lightly rings the ablation site. At 1000 magnification, these difference are quite distinct at long irradiation times, e.g. 24 and 32 s [Fig. 3(a, b)]. Under these conditions, the texture of the crater walls is very rough. In contrast, the crater wall of dry otic tissue is quite smooth [Fig. 3(d)] and similar to the morphology of the crater wall in wet tissue that has been exposed to only 11 s of irradiation.

Wet otic capsule versus wet cortical bone

A comparison of SEM findings in the crater base of wet otic and cortical bone at high-power magnification revealed several interesting differences. At 5 s, wet cortex looks like very amorphous masses of molten bone strewn across the base of the crater [Fig. 5(a)]. There is no evidence of molten bone sphere formation, although many of the structures suggest the early formation of these spheres. At 10 s of laser exposure, the surfaces of wet cortex appear different than the surfaces of wet otic tissue. Wet otic tissue (at 12 s) is smooth with an almost melted appearance [Fig. 2(b)], whereas in wet cortical tissue, there are numerous spheres of molten bone with clearly ruptured spheroids of molten bone [Fig. 6(c)].

DISCUSSION

The mechanisms of laser-mediated bone destruction are a function of several factors including the properties of the laser (wave-

length, pulse width, beam diameter, flux, angle of incidence) and the intrinsic characteristics of the tissue (surface contour, laser reflection and absorption depth, thermal diffusivity, vaporization energy, melt energy, specific heat, Gruneisen coefficient, spall strength, ionization energy) (27). Modelling of the ablation process in biological tissues is limited to simple structures, and complex heterogeneous substances such as bone have not been effectively simulated. Hence, ablation in biological tissues is often described qualitatively or in terms of gross descriptors such as ablation rates and photoacoustic transients. The pulsed i.r. laser ablation of hard tissue is thought to occur primarily by the thermal vaporization of water or organic bone constituents. Photochemical ablation would not be expected at i.r. wavelengths and the pulse widths employed in this study.

The changes that occur in biological tissues as a function of temperature are quite complicated (28): protein denaturation occurs near 60 °C and water vaporizes at 100 °C. From 100 to 300 °C, decomposition of the organic components of tissue occurs with a combination of combustion and pyrolysis resulting in the carbonization of tissue. The burning and evaporation of inorganic components occurs over a much broader temperature range. Bone has been estimated to vaporize between 300 and 1000 °C. Pure hydroxyapatite has been estimated to melt at 1670 °C. Collagen, the major organic component of bone, melts near 200 °C. The composition of bone has been estimated to be approximately 60% mineral (chiefly hydroxyapatite), 30% organic substances (collagen) and 10% water (29). The mixture of collagen, water and bone matrix ultimately results in the formation of a low-boiling-point composite material that undergoes decomposition, pyrolysis and vaporization resulting in violent ejection of both volatile and non-volatile components (29).

In this study, several general observations on the mechanisms of ablation were noted. The most striking observation was the finding of large globular spheroid masses in the bases of the ablation craters. This was a regular finding in both wet and dry tissues and under multiple exposures. Many of these structures appear to be ruptured and strongly suggest the violent release of gaseous contents within the globule. These ruptured globules are a common finding in the crater bases in both otic and cortical tissue under both wet and dry conditions. While the relative size of these globules differ between cortical and otic bone tissues, their presence in dehydrated tissue suggest that tissue components other than water are vaporized.

In dry cortical bone, another finding of note was the presence of a lattice-like pattern of small fibres after only brief laser irradiation (5 s). After further laser irradiation, this feature disappears. The size and distribution of these fibres suggests that they are collagen fibres, and the surrounding bone matrix encompassing these structures has been selectively ablated away. The absence of these findings (presumably collagen fibres) in wet cortical treated with the same laser parameters suggests that early in the ablation process in dry tissue, an amalgam of organic and inorganic components of bone (hydroxyapatite) is preferentially ablated away. It is unlikely that hydroxyapatite was vaporized as its melting temperature has been estimated to be near 1670 °C.

Mid-i.r. wavelengths in bone ablation have not been studied extensively by scanning electron microscopy. In contrast, SEM on laser-treated hard dental tissues has been an area of extensive investigation for years. The structures in teeth share great similarity to bone in that they are composed of hydroxyapatite, water and proteins in similar distributions as that encountered in bone tissue. CO_2 laser irradiation of tooth enamel has demonstrated the differential ablation of the organic components of the tissue resulting in an increase in the mineral content of surface (30). The increase in the mineral content of the surface relative to the protein component has been confirmed by several methods and seen with other lasers including Nd-YAG (31). Both CO_2 and Nd-YAG lasers have caused the fusion of enamel and dentine with the melting and recrystallization of the mineral elements of teeth (32, 33). The surface features produced by a given laser vary considerably with energy density. Indeed, in earlier studies on the effects of excimer lasers on dentine we observed selective surface ablation of intertubular dentine, peritubular dentine or simply uniform 'coating of the crater bottom by a melted layer of hydroxyapatite' (34, 35).

With a longer wavelength excimer (XeCl at 308 nm) we have observed the formation of globules of re-solidified hydroxyapatite over the dentine tubules similar to the globules of melted bone in this study (36). These went on

to burst as fluence increased to 4 and 7 J cm $^{-2}$. Since the absorption characteristics of the excimer and the Ho-YAG laser are different, the ablation characteristics would also be expected to be different. However, the formation of these structures from re-solidified matrix material may arise from similar mechanisms.

Also in dentine Stern et al (33) noted the presence of large cracks, small fissures, and pores in CO_2 treated tissue. Notably, the number of pores on the laser-treated surfaces decreased with lower energy densities. At high densities pores as large as 1 μm were observed. Pores and minute surface cracks were observed in otic tissues in this study and bear similarity to the observation noted in teeth (33).

Finally, while we emphasized the difference in structure, the observed differences in ablation crater morphology between otic capsule bone and cortical bone cannot be easily accounted for by one factor alone. Several factors contribute to these differences. The most obvious is the difference in microarchitecture between cortical bone, which has a porous structure resembling coarse ceramic, and otic capsule, which is smooth and relatively homogeneous. Otic capsule and cortical bone may also differ in composition. While collagen and hydroxyapatite are the major non-aqueous constituents of bone, their relative proportions may differ between the two tissues. Furthermore, the type of collagen in the embryologically primitive otic capsule may differ substantially from that found in other bony tissues.

CONCLUSIONS

A regular finding of globular spheroids of material, probably created by the formation of bone matrix or water to gaseous phase, was noted in both wet and dried specimens in both tissues. Several of these globules ruptured yielding an SEM image which suggests a violent process whereby the inner contents are ejected. In the ablation of dry bone, SEMs of tissues treated for short periods of time demonstrated the presence of fibrous structures. This may reflect the selective removal of surface bone constituents with preservation of subsurface residual collagen fibres. These disappear with longer laser irradiation times. In regions where the energy density during irradiation is near or below threshold, subtle differences between wet and dry tissue were noted. The ablation crater walls in wet tissues appear rougher and possibly reflect a more violent ablation process suggestive of water vaporization causing expulsion of bone material. In contrast, the crater walls in dry tissue appear smoother.

ACKNOWLEDGEMENTS

We thank Bill Walker of the Clougherty Packing Company for his assistance with tissue specimens, and Petra Wilder-Smith DDS PhD, Mark R. Dickinson PhD and Karen J. Doyle MD PhD for their comments and review of the manuscript. This work was supportd by the following grants: ONR N0014-91-C-0134, DOE DE-FG03-91ER61227 and NIH 5P41RR01192. Dr Wong is supported by the Research Fund of the American Otological Society.

REFERENCES

1 Perkins RC. Laser stapedotomy for otosclerosis. *Laryngoscope* 1980, **90**:228–41

2 Causse J-B, Gherini S, Horn KL. Surgical treatment of stapes fixation by fiberoptic argon laser stapedotomy with reconstruction of the annular ligament. *Otolaryngol Clin N Am* 1993, **26**:395–416

3 Gherini S, Horn KL, Causse J-B, McArthur GR. Fiberoptic argon laser stapedotomy: is it safe? *Am J Otol* 1993, **14**:283–9

4 Lesinski SG, Newrock R. Carbon dioxide lasers for otosclerosis. *Otolaryngol Clin N Am* 1993, **26**:417–41

5 Thedinger BS. Applications of the KTP laser in chronic ear surgery. *Am J Otol* 1990, **11**:79–84

6 Silverstein H, Rosenberg S, Jones R. Small fenestra stapedotomies with and without KTP laser: a comparison. *Laryngoscope* 1989, **99**:485–8

7 Bartels LJ. KTP laser stapedotomy: is it safe? *Otolaryngol Head Neck Surg* 1990, **103**:685–92

8 Kautzky M, Trodhan A, Susani M, Schenk P. Infrared laser stapedotomy. *Eur Arch Otorhinolaryngol* 1991, **248**:449–51

9 Foth H-J, Barton T, Horman K et al. Possibilities and problems of using the holmium laser in ENT. *Proc SPIE* 1994, **2128**:17–23

10 Stubig IM, Reder PA, Facer GW et al. Holmium-YAG laser stapedotomy: preliminary evaluation. *Proc SPIE* 1993, **1876**:10–6

11 Nuss RC, Fabian RL, Sarkar R, Puliafito CA. Infrared laser bone ablation. *Lasers Surg Med* 1988, **8**:381–91

12 Bast T. Ossification of the otic capsule in human fetuses. *Contrib Embryol* 1930, **21**:53–82

13 Wiet RJ, Causse J-B, Shambaugh J, Causse JR. *Otosclerosis (Otospongiosis)*. Alexandria, Virginia: American Academy of Otolaryngology-Head and Neck Surgery Foundation, 1991

14 Fawcett D. *A Textbook of Histology*. Philadelphia: Saunders, 1986

15 Wong B, Neev J, Cheung E, Berns M. Pulsed infrared laser ablation rates and characteristics in otic capsule. *Proc SPIE* 1995, **2395**:285–95
16 Walsh JT, Deutsch TF. Er-YAG laser ablation of tissue: measurement of ablation rates. *Lasers Surg Med* 1989, **9**:327–37
17 Walsh J, Hill D. Erbium laser ablation of bone: effect of water content. *Proc SPIE* 1991, **1427**:27–33
18 Neev J, Wong B, Lee J et al. The effect of water content on UV and IR laser ablation of hard tissues. *Proc SPIE* 1994, **2323**:292–300
19 Neev J, Lee J, Cheung E. Effect of water content on hard dental tissue ablation (submitted)
20 Wong BJF, Neev J, Sung V, Berns MW. Holmium-YAG laser ablation characteristics in calvarial lamellar and cortical bone: the role of water and tissue microarchitecture. Proc SPIE (in press)
21 Harada Y. *Atlas of the Ear by Scanning Electron Microscopy*. Baltimore, Maryland: University Park Press, 1983
22 Lim DJ. A scanning electron microscopic investigation on otosclerotic stapes. *Ann Otol Rhinol Laryngol* 1970, **79**:780–99
23 Kluyskens P, Fiermans L, Dekeyser W, Vakaet L. Scanning electron microscopic studies of the stapes in normal and in some pathological experimental conditions. *Acta Otolaryngol* 1976, **81**:220–7
24 Graham MD, Perkins R. A scanning electron microscopic study of the normal human stapes. *Ann Otol Rhinol Laryngol* 1978, **88**:2–14
25 Segas J, Georgiadis A, Christodoulou P et al. Use of the excimer laser in stapes surgery and ossiculoplasty of middle ear ossicles: preliminary report of an experimental approach. *Laryngoscope* 1991, **101**:186–91
26 Schlenk E, Profeta G, Nelson JS et al. Laser assisted fixation of ear prosthesis after stapedectomy. *Lasers Surg Med* 1990, **10**:444–7
27 Dingus R. Laser-induced shock wave effects in materials. *Proc SPIE* 1990, **1202**:36–45
28 Verdaasdonk RM, Borst C, van Gemert MJC. Explosive onset of continuous wave laser tissue ablation. *Phys Med Biol* 1990, **35**:1129–44
29 Izatt JA, Sankey ND, Partovi F et al. Ablation of calcified biological tissue using pulsed hydrogen fluoride laser radiation. *IEEE J Quant Electron* 1990, **26**:2261–70
30 Kantola S. Laser-induced effects on tooth structure IV: a study of changes in the calcium and phosphorous contents in dentine by electron probe microanalyis. *Acta Odont Scand* 1972, **30**:463–74
31 Spencer P, Trylovich DJ, Cobb CM. Chemical characterization of lased root surfaces using fourier transform infrared photoacoustic spectroscopy. *J Periodontol* 1992, **63**:633–6
32 Dederich DN, Zakariasen KL, Tulip J. Scanning electron microscopic analysis of canal wall dentin following neodymium-yttrium-aluminum-garnet laser irradiation. *J Endodont* 1984, **10**:428–31
33 Stern RH, Vahl J, Sognnaes RF. Lased enamel: ultrastructural observations of pulsed carbon dioxide laser effects. *J Dent Res* 1972, **51**:455–60
34 Neev J, Liaw LL, Raney DV et al. Selectivity and efficiency in the ablation of hard dental tissue with ArF pulsed excimer lasers. *Lasers Surg Med* 1991, **11**:499–510
35 Neev J, Raney DV, Whalen WE et al. Ablation of hard dental tissues with ArF pulsed excimer laser. *Proc SPIE* 1991, **1427**:162–72
36 Neev J, Stabholtz A, Liaw L-HL et al. Scanning electron microscopy and thermal characteristics of dentin ablated by a short-pulse XeCl excimer laser. *Lasers Surg Med* 1993, **13**:353–62

Key words: Bone histology; Scanning electron microscopy; Holmium-YAG laser; Infra-red lasers; Laser surgery; Photoablation; Stapes